Perpendicular magnetic anisotropies in ultrathin BCC iron films and surfaces

1994 J. Phys.: Condens. Matter 6 1183

(http://iopscience.iop.org/0953-8984/6/6/021)

J. Phys.: Condens. Matter 6 (1994) 1183–1206. Printed in the UK

Perpendicular magnetic anisotropies in ultrathin BCC iron films and surfaces

Long-Pei Shi

Microelectronics Research Institute of Zhongshan University, Guangzhou, People's Republic of China

Received 14 January 1992, in final form 6 September 1993

Abstract. The perpendicular magnetic anisotropy in one- to six-monolayer BCC Fe films is studied by the Green-function method based upon the Heisenberg model ($S \geqslant 1$) with out-of-plane spin orientation of the atoms at the surfaces. The various anisotropy constants resulting from surface single-ion anisotropy have been derived for the first time. According to the anisotropy constants as functions of the thickness of ultrathin films and temperature, we explain that there is a perpendicular remanence for an intermediate range of thickness of ultrathin films and temperature. The Curie temperature and the spontaneous magnetization of each atomic plane are calculated by taking into account the exchange interaction of the first- and second-neighbour couplings. It has been shown that in a one-monolayer film the second-neighbour exchange coupling was enhanced markedly owing to loss of the first-neighbour atoms and great enhancement of the overlap of the electron cloud of the second-neighbour atoms. It is proved that the behaviours of ferromagnetic transition and perpendicular remanence of ultrathin films depend strongly on the requirement that the spin be perpendicularly pinned to some degree at the surfaces.

1. Introduction

Recent experiments were exploited to study epitaxial BCC Fe films grown on Ag(001), Au(001) and Pd(001) (abbreviated Fe/Ag(001), Fe/Au(001) and Fe/Pd(001)). It has been shown that the perpendicular magnetic behaviour in ultrathin films points out the observed discrepancies between various experiments. (i) The work of Jonker *et al* [1] has shown that at room temperature there was no in-plane moment for films less than three monolayers (ML). It was suggested that this resulted from a perpendicular anisotropy strong enough to compete with the demagnetization field, which forced the magnetic moments to lie along the surface normal. (ii) Koon *et al* [2] showed that at temperatures down to 15 K the orientation of the magnetic moment of 1 and 2.4 ML films in zero applied field is perpendicular to the film plane, while the orientation of the 5.5 ML sample is in-plane at room temperature and partially out-of-plane at low temperature. (iii) The work of Stampanoni *et al* [3] has shown that at $T = 30$ K the 3 to 4 ML films have a perpendicular remanence (PR), whereas thinner and thicker films have their magnetization in-plane. Above $T = 100$ K no PR has been observed for any film thickness. (iv) Cabanel *et al* [4] showed that for the BCC Fe(001)/FCC Ag(001) superlattices the interface anisotropy overcomes the demagnetizing field effect when the thickness of the Fe layers decreases below 10 Å ($\simeq 7$ ML). From magnetization measurements, the anisotropy for the 50×(10 Å Fe/40 Å Ag) superlattice is perpendicular at 5 K and in-plane at 300 K. The anisotropy constant is derived from both experiments, which leads to 0.8 erg cm^{-2} for the interface anisotropy constant K_s.

0953-8984/94/061183+24$07.50

Although there are quite a few discrepancies in the results of the above-mentioned experiments, it shown that the PR of ultrathin films depends strongly on the temperature and the thickness of ultrathin films. In this paper, we give a theoretical interpretation of the discrepancies in the results of various experiments based upon the surface anisotropy (SA) of BCC Fe film [5]. As Pappas [6] and Rau *et al* [7] remark, the observed discrepancies between various experimental results could be due to effects caused by surface oxygen absorption and coatings, or stress and strain in films evaporated at different temperatures, or the use of non-atomically flat substrate surfaces resulting in stepped films. We introduce the strength of surface anisotropy D to describe the surface situation of various experimental specimens. The theory shows that the discrepancies of SA strongly change the behaviour of PR of ultrathin films. The observed discrepancies between various experimental results could be explained by the discrepancies of SA of various experimental specimens.

Recent studies have shown that the ferromagnetic phase transition in ultrathin films and surfaces may differ markedly from that in the bulk. The experiments were exploited to study Fe/Ag(001), Fe/Au(001) and Fe/Pd(001) films. It has been shown that the magnetic phase transition behaviour of ultrathin films is not the same as that of a bulk magnet: Very thin magnetic films—in the case of BCC Fe/Ag(001) < 5 ML—have a reduced transition temperature [8]. Fe/Ag(001) films thicker than 5 ML have a Curie temperature T_C equal to that of bulk BCC Fe, while T_C of a 1 ML film is about 400 K [3]. Rau *et al* [7] have shown that the Curie temperature of a 1 ML Fe/Ag(001) film is below 290 K. Durr *et al* [9] studied the system Fe/Au(001), and found that the Curie temperature of a 1 ML film is 300 K, that of a 2 ML film is 400 K and that of a 3 ML is 600 K; for thickness larger than 1 ML the bulk value is rapidly approached. Liu *et al* [10] studied magnetic properties of the system Fe/Pd(001). Their experiments showed that there is a rapid change in the T_C values in the monolayer and submonolayer region and a more gradual change for thicker films: While T_C of a 1 ML film is just above 300 K, T_C of a 2 ML film is 500 K and T_C of a 4 ML film is 600 K.

We have recently studied the ferromagnetic phase transition in ultrathin films [11] and multilayer films [12] for simple cubic lattices. In this paper we use a similar method to study BCC Fe ultrathin films. The expression for the Curie temperature as a function of the thickness of ultrathin films and the surface anisotropy have been derived. The agreement between calculation and experiment is remarkably good.

2. Model

Gay *et al* [5] calculated the spin anisotropy of monolayers of Fe, Ni, V and Co by incorporating the spin–orbit interaction into the self-consistent local-orbital method. They found that the easy direction of magnetization is perpendicular to the plane of the monolayer for Fe and V, but in the plane for Ni and Co. In terms of energy per atom, the monolayer anisotropies are large. For example, the anisotropy of the Fe monolayer ($\simeq 0.4$ meV/atom) is 100 times the anisotropy of bulk Fe (4 μeV/atom). This is a consequence of the reduced symmetry of the monolayers, which allows the anisotropy to enter in second order. To study the effect of surface on the nature of the ferromagnetic phase transition and perpendicular magnetic anisotropy, we assume that the surfaces of BCC Fe n ML films are parallel to (001) planes and perpendicular to the z axis. The films have a finite amount of n atomic planes in the z [001] direction and an infinite number of N atoms ($N \to \infty$) in both the x [100] and y [010] direction. We shall use two different coordinate systems: the system (x, y, z) is related to the lattice, the z axis being perpendicular to the film plane;

and the system (X, Y, Z) refers to the spins, with Z being the quantization axis. For the perpendicular easy axis the two systems coincide; whereas for easy-plane anisotropy, Z coincides with y (X with z, and Y with x). The spin Hamiltonian of a BCC Fe film contains three parts: the Heisenberg exchange term, the shape anisotropy (demagnetization) term and the surface anisotropy (SA) term. To consider incorporating the spin–orbit interaction into the local orbital [5] and demagnetization energy of uniform magnetization, these terms can be deduced by the method of second quantization. The spin Hamiltonian is given by

$$\mathcal{H} = -\frac{1}{2}\sum_{\alpha, f_1, f_2} J_{f_1 f_2} S^{\alpha}_{f_1} S^{\alpha}_{f_2} - \sum_{f} D_f (S^z_f)^2 + \frac{\mu^2}{2V} N_z \sum_{f_1, f_2} S^z_{f_1} S^z_{f_2}. \tag{1}$$

Here lattice site f stands for the position vector j in the xy plane and the coordinate ν in the z direction $f = (j, \nu)$; ν marks the atomic planes of the n ML films ($\nu = 1, 2, 3, \ldots, n$); and α denotes x, y and z. The exchange interaction of the first-neighbour coupling ($J_{f_1 f_2} = J_f$) and the second-neighbour coupling ($J_{f_1 f_2} = J_s$) are taken into account. For simplicity, we assume that the n ML films have a symmetrical surface and the spin orientation of the atoms in the surfaces is out-of-plane, i.e. D_f takes the values $D_f = D_\nu = 0$ (for $\nu = 2, 3, \ldots, n-1$) and $D_1 = D_n = D > 0$, in which the strength of surface anisotropy D measures the fact that the spin be perpendicularly pinned to some degree at the surface. In order that this Hamiltonian may give an SA term, it is necessary that $S \geqslant 1$, where S denotes the quantum number of the spin operator. N_z denotes the perpendicular demagnetization factor; N_x and N_y are the plane demagnetization factors in ultrathin film. Let $N_z = 4\pi$, $N_x = N_y = 0$ approximately. V is the volume of the film, v is the primitive cell volume ($V = N^2 n v$). μ is magnetic moment; μS is magnetic moment of an atom. Values appropriate for iron are $S = 1$, $\mu = 2.2\mu_B$ and Bohr magneton $\mu_B = 0.927 \times 10^{-20}$ erg Oe^{-1}.

We study ultrathin films with perpendicular surface anisotropy energy and demagnetization energy, as shown in equation (1). The film has uniaxial anisotropy, and thus the orientations of spontaneous magnetization (the direction of order for spins) in ultrathin films are all the same, either perpendicular to the film plane for the perpendicular easy axis or in the film plane for the easy-plane anisotropy, while the magnitude of spontaneous magnetization (the degree of order for spins) changes with the position of the atomic planes owing to loss of translational invariance in one direction of the ultrathin films [11, 12]. In ultrathin films the presence of the ferromagnetic domain structure is possible [13]; this case is not discussed in this paper.

3. Curie temperature T_C and spontaneous magnetization σ_ν of each atomic plane in BCC films

This section examines the relative magnetization σ_f at site f in the case of perpendicular easy axis, for which the two coordinate systems (x, y, z) and (X, Y, Z) coincide. Because the Z axis is the axis of quantization, we have $\langle S^z_f \rangle = \sigma_f S$, in which $\langle\ \rangle$ denotes the statistical average. To take into account the translational invariance along the XY plane, σ_f will depend only on the position ν involved, so that $\sigma_f = \sigma_\nu$. The present paper is concerned primarily with finding a statistical approximation that is able to describe the magnetic anisotropy of a ferromagnetic film in the presence of surface single-ion anisotropy. In order to treat the single-ion anisotropy by the double-time Green-function method, decoupling procedures are generally employed to reduce the higher-order functions to the original Green function. The exchange function can be decoupled by the Tyablikov approximation:

$\langle\langle S_f^Z S_h^+ | B_g \rangle\rangle \simeq \langle S_f^Z \rangle \langle\langle S_h^+ | B_g \rangle\rangle$ for $f \neq h$. This is certainly a reasonable approximation as long as $f \neq h$. For the special case $f = h$, such an approximation is less valid. Nevertheless there have been three distinct attempts to decouple the anisotropy Green function. They are each of the form $\langle\langle S_f^Z S_f^+ + S_f^+ S_f^Z | B_g \rangle\rangle \simeq \Gamma_f \langle S_f^Z \rangle \langle\langle S_f^+ | B_g \rangle\rangle$. The three choices made for Γ_f have been as follows:

Shi [11]

$$\Gamma_f = 1$$

Anderson and Callen [14]

$$\Gamma_f = 2 - (1/2S^2)\langle S_f^- S_f^+ + S_f^+ S_f^- \rangle$$

Lines [15]

$$\Gamma_f = \langle 3(S_f^Z)^2 - S(S+1) \rangle / \langle S_f^Z \rangle^2 \qquad \text{for } B_g = S_g^-$$

$$\Gamma_f = \frac{\langle 2(S_f^Z)^4 + 3(S_f^Z)^3 - (2S^2 + 2S - 1)(S_f^Z)^2 - S(S+1)S_f^Z \rangle}{\langle S_f^Z \rangle \langle (S_f^Z)^3 + (S_f^Z)^2 - S(S+1)S_f^Z \rangle} \qquad \text{for } B_g = S_g^Z S_g^-.$$

Devlin [16] has set up a new formalism in which it is not necessary to decouple the anisotropy Green functions and employ the decoupling schemes of the exchange terms. Quantitative calculations are carried out for the Cure temperature of body-centred cubic lattices with $S = 1$, which corresponds to the iron lattice. Although the decoupling scheme given by Devlin does remarkably well in comparison with the earlier theories on this subject, the results for the above different theories are approximately all the same in the case of small D ($D/J \leqslant 0.5$) [16].

A ferromagnetic thin film with the single-ion anisotropy has been studied by Endo and Ayukawa [17] using the Green-function method and Devlin's decoupling scheme for the whole range of anisotropy strengths. In this paper we discuss the single-ion anisotropy of the iron ultrathin film ($S = 1$) for D very small ($D/J \ll 0.5$). In order to simplify the calculation for the spontaneous magnetization and conform with the calculation for the anisotropic constant (see equation (12)), the decoupling scheme choice made for Γ_f has been such that (see (9*d*)):

$$\Gamma_f = \langle 3(S_f^Z)^2 - S(S+1) \rangle / \langle S_f^Z \rangle^2 = [2S(S+1) - 3(1 + 2P_\nu)\langle S_\nu^Z \rangle] / \langle S_\nu^Z \rangle^2.$$

From 0 K to the Curie point the values of Γ_f as a function of temperature are from 1 to 3/4 for the above decoupling scheme, from 1 to 2/3 for the Anderson and Callen decoupling scheme and 1 for Shi's decoupling scheme respectively.

From (1) we have [11]

$$S\sigma_\nu = \frac{(S - P_\nu)(1 + P_\nu)^{2S+1} + (1 + S + P_\nu)P_\nu^{2S+1}}{(1 + P_\nu)^{2S+1} - P_\nu^{2S+1}}. \tag{2}$$

3.1. For BCC n ML films ($n \geqslant 2$)

In this case

$$P_\nu = \frac{1}{(2\pi)^2}\int\int_{-\pi}^{\pi} \mathrm{d}h_x\,\mathrm{d}h_y \sum_{k=1}^{n} \frac{U_{\nu k}^2}{\exp(\omega_{hk}/k_\mathrm{B}T)-1} \tag{3}$$

$$P_\nu = P_{n+1-\nu}$$

where k_B is Boltzmann's constant and T is absolute temperature. ω_{hk} is determined by the characteristic equation as follows:

$$\begin{vmatrix} \omega_{hk}-E_1 & J_1 & J_1' & & & & & \\ J_2 & \omega_{hk}-E_2 & J_2 & J_2' & & & & \\ & & \ddots & & & & & \\ & J_\nu' & J_\nu & \omega_{hk}-E_\nu & J_\nu & J_\nu' & & \\ & & & & \ddots & & & \\ & & & J_2' & J_2 & \omega_{hk}-E_2 & J_2 & \\ & & & & J_1' & J_1 & \omega_{hk}-E_1 & \end{vmatrix} = 0 \tag{4}$$

$$E_1 = 4J_f S\sigma_2 + 2J_s S\sigma_1(2-\cos h_x - \cos h_y) + J_s S\sigma_3 + D\Gamma_1 S\sigma_1 - \mu 4\pi M_s$$

$$\vdots$$

$$E_\nu = 4J_f S(\sigma_{\nu-1}+\sigma_{\nu+1}) + 2J_s S\sigma_\nu(2-\cos h_x - \cos h_y) + J_s S(\sigma_{\nu-2}+\sigma_{\nu+2}) - \mu 4\pi M_s \qquad (\text{for } \nu = 2,\ldots,n-1) \tag{4a}$$

$$J_\nu = 4J_f S\sigma_\nu \cos(h_x/2)\cos(h_y/2) \qquad J_\nu' = J_s S\sigma_\nu \qquad (\text{for } \nu = 1,\ldots,n) \tag{4b}$$

$$\Gamma_1 = [2S(S+1) - 3(1+2P_1)S\sigma_1]/(S\sigma_1)^2 \tag{4c}$$

$$M_s = \mu\sum_f \langle S_f^Z\rangle / V = M_s(0)\frac{1}{n}\sum_\nu \sigma_\nu \qquad M_s(0) = \mu S/v \tag{4d}$$

$$\sigma_\nu = \sigma_{n+1-\nu} \qquad E_\nu = E_{n+1-\nu}$$

$$\omega_{hk} \text{ and } U_{\nu k}^2 = A_{\nu\nu}(\omega_{hk})/\Pi_{L(\neq k)}(\omega_{hk}-\omega_{hL}) \qquad (\text{see appendix}) \tag{4e}$$

$$h_x = 2\pi n_x/N \qquad h_y = 2\pi n_y/N$$

where the allowed values of n_x and n_y are $0, \pm1, \pm2, \ldots \pm N/2$ ($N \to \infty$), k and L take the values $1, 2, 3, \ldots, n$. $A_{\nu\nu}(\omega_{hk})$ is the subdeterminant of the ν row, ν column of the tridiagonal form (4).

Using (2)–(4*e*), we can calculate the Curie temperature $T_{\mathrm{C}\nu}$ and the temperature dependence of the spontaneous magnetization σ_ν ($\nu = 1, 2, 3, \ldots, n$). For inequivalent atomic planes of n ML films the σ_ν are different but $T_{\mathrm{C}\nu}$ are equal [11].

Otherwise, from (2)–(4*e*) and the high-temperature approximation [18] we deduce the Curie temperature of atomic planes in the film:

$$T_{\mathrm{C}\nu} = [8S(S+1)/3C_\nu](J_f/k_\mathrm{B}) \tag{5}$$

where

$$C_\nu = \frac{1}{(2\pi)^2}\int\int_{-\pi}^{\pi} \mathrm{d}h_x\,\mathrm{d}h_y \sum_{k=1}^{n} \frac{8S\sigma_\nu J_f U_{\nu k}^2}{\omega_{hk}} \tag{6}$$

$$C_\nu = C_{n+1-\nu} \qquad T_{C\nu} = T_{Cn+1-\nu} \qquad (\nu = 1, 2, \ldots, n).$$

Because ω_{hk}/σ_ν depends on σ_μ/σ_ν (see (4) and appendix), the convergent condition of integrals (6) requires that the values of σ_ν/σ_μ are finite and non-zero or σ_ν ($\nu = 1, 2, 3, \ldots, n$) simultaneously approaches zero at the Curie temperature T_C, i.e. the Curie temperatures of atomic planes in n ML films are equal:

$$T_C = T_{C1} = T_{C\nu}$$

or

$$C_1 = C_\nu \qquad (\nu = 2, 3, \ldots, n/2 \text{ or } (n+1)/2). \tag{7}$$

To satisfy the condition (7) the Curie temperature T_C and the ratio of σ_1 and σ_ν ($\nu = 2, 3, \ldots, n$) has been determined simultaneously by the use of (5) and (6). When the above-discussed different methods for determining the Curie temperatures are compared, their results are consistent [11, 12].

3.2. For BCC 1 ML films

This is two-dimensional square lattice with the exchange integral $J_{f_1 f_2} = J_s$. Equations (2) and (3) can be replaced by

$$\sigma_\nu = \sigma_1$$

$$P_\nu = P_1 = \frac{1}{(2\pi)^2}\int\int_{-\pi}^{\pi} \mathrm{d}h_x\,\mathrm{d}h_y \frac{1}{\exp(\omega_{h1}/k_B T) - 1}. \tag{3a}$$

The Curie temperatue of 1 ML films is given by

$$T_C = [4S(S+1)/3C_1](J_s/K) \tag{5a}$$

where

$$C_1 = \frac{1}{(2\pi)^2}\int\int_{-\pi}^{\pi} \mathrm{d}h_x\,\mathrm{d}h_y \frac{4S\sigma_1 J_s}{\omega_{h1}} \tag{6a}$$

$$\omega_{h1} = 2J_s S\sigma_1(2 - \cos h_x - \cos h_y) + D\Gamma_1 S\sigma_1 - \mu 4\pi M_s(0)\sigma_1.$$

3.3. *For BCC bulk magnet*

This corresponds to films with $n \to \infty$. The Curie temperature T_{Cb} is given by

$$T_{Cb} = [8S(S+1)/3C_b](J_f/k_B) \tag{8}$$

where

$$C_b = \frac{1}{(2\pi)^3}\int\int\int_{-\pi}^{\pi} \mathrm{d}h_x\,\mathrm{d}h_y\,\mathrm{d}h_z/\omega_h \tag{8a}$$

$$\omega_h = 1 - \cos(h_x/2)\cos(h_y/2)\cos(h_z/2) + (3J_s/4J_f)[1 - (\cos h_x + \cos h_y + \cos h_z)/3].$$

Finally, we must emphasize that the calculated formulae for the spontaneous magnetization (the integral (3) or (3*a*) can be integrated at finite temperature τ) given by this section are suitable only for the case of perpendicular easy axis. Whether there is an energy gap at the bottom of the spin-wave spectrum decides the convergence of integral (3) or (3*a*) and the magnetization state in n ML film. The stabilization of perpendicular magnetization in this case is due mainly to the surface anisotropy (SA) and to the associated gap at the bottom of the spin-wave spectrum (see appendix). It is consistent with the criterion of PR, i.e. the presence of an energy gap is equivalent to $K_u(\tau) > 0$ (see the next section). For the case of very weak SA the dipolar interaction is large compared to SA and no gap appears at the bottom of the spin-wave spectrum. Therefore the integral (3) or (3*a*) cannot be integrated. This shows that the magnetization is stabilized in-plane and no longer lies along the surface normal, which corresponds to $K_u(\tau) < 0$. If the energy gap of the bottom of the spin-wave spectrum equals zero at the temperature τ_r and $K_u(\tau_r) = 0$ (see the next section), the integral (3) or (3*a*) cannot be integrated, which means that a reversible transition between in-plane and perpendicular magnetization exists in the n ML film at the temperature τ_r (τ_r is called the transition point). If the integral (6) or (6*a*) can be integrated, it means that from 0 K to the Curie point there is a PR in the n ML film. Conversely, if the integral (6) or (6*a*) cannot be integrated, this shows that from 0 K to the Curie point or at least in the range of high temperature there is in-plane magnetization PR.

4. Perpendicular magnetic anisotropies in ultrathin BCC films

We examine the perpendicular magnetic anisotropy in ultrathin films. The assumption is made that the magnetic anisotropy energy depends on the direction of spontaneous magnetization γ with respect to the film or lattice axes (x[100], y[010], z[001]), that is on the direction cosines $\gamma^x, \gamma^y, \gamma^z$. We assume new axes (X, Y, Z) in which Z is the direction of the spontaneous magnetization (Z being the quantization axis) and θ is the angle between z and Z axes. Let the components of the spin operator with respect to the film axes be S^x, S^y, S^z and to the new axes be S^X, S^Y, S^Z. Tyablikov [18] gave their transformation relation:

$$S_f^\alpha = \gamma^\alpha S_f^Z + A^\alpha S_f^+ + A^{\alpha *} S_f^- \qquad S_f^+ = S_f^X + \mathrm{i}S_f^Y \qquad S_f^- = S_f^X - \mathrm{i}S_f^Y \tag{9}$$

where

$$\alpha = x, y, z \qquad \gamma^z = \cos\theta \qquad A^z = \tfrac{1}{2}[1 - (\gamma^z)^2]^{1/2}$$
$$\gamma^x\gamma^x + \gamma^y\gamma^y + \gamma^z\gamma^z = 1 \qquad A^x\gamma^x + A^y\gamma^y + A^z\gamma^z = 0 \tag{9a}$$
$$A^xA^x + A^yA^y + A^zA^z = 0 \qquad A^{x*}A^x + A^{y*}A^y + A^{z*}A^z = 1/2.$$

Substitution of (9) and (9*a*) into (1) leads to the expression for the spin Hamiltonian and the free energy of the system F or f

$$\mathcal{H} = \frac{1}{2}\sum_{f_1 f_2} J_{f_1 f_2}(S_{f_1}^Z S_{f_2}^Z + S_{f_1}^+ S_{f_2}^-) - \sum_f D_f[(\gamma^z)^2(S_f^Z)^2 + (A^z)^2(S_f^+)^2 + (A^{z*})^2(S_f^-)^2$$
$$+ \gamma^z A^z(S_f^Z S_f^+ + S_f^+ S_f^Z) + \gamma^z A^{z*}(S_f^Z S_f^- + S_f^- S_f^Z)$$
$$+ A^z A^{z*}(S_f^+ S_f^- + S_f^- S_f^+)] + \ldots \tag{1a}$$

$$F = F_{ex} + F_k + F_d = -k_B T \ln \mathrm{sp}(\mathrm{e}^{-\mathcal{H}/k_B T}) \qquad f = F/V \tag{10}$$

where F_{ex} is the exchange energy, F_k is the crystalline anisotropy energy and F_d is the shape anisotropy (demagnetization) energy.

The free energy f and the uniaxial anisotropy constant K_u are given by

$$f = f_0 + K_u \sin^2\theta + \ldots$$
$$K_u = \frac{1}{V}\frac{\partial F}{\partial(\sin^2\theta)} = \frac{1}{V}\left\langle\frac{\partial \mathcal{H}}{\partial(\sin^2\theta)}\right\rangle = K_v - K_d. \tag{11}$$

We define the crystalline anisotropy constant or the effective volume anisotropy constant K_v and the shape anisotropy constant K_d.

Because the Z axis is the axis of quantization, so $\langle S_f^X\rangle = \langle S_f^Y\rangle = 0$, $\langle S_f^+\rangle = \langle S_f^-\rangle = 0$. By employing the Green-function method [18], we have

$$\langle(S_f^+)^2\rangle = \langle(S_f^-)^2\rangle = \langle S_f^+ S_f^Z\rangle = \langle S_f^- S_f^Z\rangle = \langle S_f^Z S_f^+\rangle = \langle S_f^Z S_f^-\rangle = 0. \tag{9b}$$

The expressions have been given by [18]

$$\langle S_f^+ S_f^- + S_f^- S_f^+\rangle = 2[S(S+1) - \langle(S_f^Z)^2\rangle] \tag{9c}$$

$$\langle(S_f^Z)^2\rangle = S(S+1) - (1+2P_f)\langle S_f^Z\rangle \tag{9d}$$

where $P_f = P_\nu$ and $\langle S_f^Z\rangle = \langle S_\nu^Z\rangle = S\sigma_\nu$ to be calculated from (2) and (3). Substituting (1*a*) and (9*a*)–(9*d*) into (11), K_v is given by

$$K_v = \frac{N^2}{V}\sum_\nu D_\nu[3\langle(S_\nu^Z)^2\rangle - S(S+1)]/2 = \frac{N^2}{V}\sum_\nu D_\nu[S(S+1) - \tfrac{3}{2}(1+2P_\nu)S\sigma_\nu] \tag{12}$$

where $V = N^2 n a^3/2$, a is the lattice constant, n is the number of atomic planes of the film and the primitive cell volume v is $a^3/2$.

Suppose the perpendicular magnetic anisotropy only resulted from the SA, i.e. $D_1 = D_n = D$, $D_\nu = 0$ ($\nu = 2, \ldots, n-1$). From equation (12) we have

$$K_s(\tau) = (D/a^2)[S(S+1) - \tfrac{3}{2}(1+2P_1)S\sigma_1] \tag{13}$$

$$K_v(\tau) = (2AD/a^3 n)[S(S+1) - \tfrac{3}{2}(1+2P_1)S\sigma_1] = (AD/a^3 n)\Gamma_1(S\sigma_1)^2 \tag{14}$$

$$K_v(\tau) = AK_s(\tau)/d \qquad d = na/2$$

where A is the number of surfaces ($A = 1$ for $n = 1$; $A = 2$ for $n \geqslant 2$), the dependence of the effective volume anisotropy constant on temperature τ has been emphasized by writing $K_v(\tau)$, while $K_s(\tau)$ is the surface anisotropy constant at temperature τ.

At absolute zero temperature, since $\sigma_1 = 1$ and $P_1 = 0$ as $\tau = 0$, equations (13) and (14) are replaced by

$$K_s(0) = (DS/a^2)(S - 1/2) \tag{13a}$$

$$K_v(0) = (2ADS/a^3 n)(S - 1/2). \tag{14a}$$

Just below the Curie temperature τ_C, since $\sigma_\nu \to 0$ and $P_\nu \to \infty$ as $\tau \to \tau_C$, equation (2) is replaced by

$$3P_\nu\sigma_\nu = (S+1)\left(1 - \tfrac{1}{2}P_\nu^{-1} + \frac{9 - 2S - 2S^2}{30}P_\nu^{-2}\ldots\right)$$

On substituting into (13) and (14) we now get

$$K_s(\tau) = \frac{D}{a^2}\left(\frac{3S(S+3/2)(S-1/2)}{5(S+1)}\sigma_1^2 + O(\sigma_1^3) + \ldots\right) \tag{13b}$$

$$K_v(\tau) = \frac{2AD}{a^3 n}\left(\frac{3S(S+3/2)(S-1/2)}{5(S+1)}\sigma_1^2 + O(\sigma_1^3) + \ldots\right). \tag{14b}$$

From (11) we derive the expression for the shape anisotropy constant $K_d(\tau)$ as:

$$K_d(\tau) = 2\pi M_s^2(\tau) = 2\pi M_s^2(0)\left(\frac{1}{n}\sum_\nu \sigma_\nu\right)^2 \tag{15}$$

where $M_s(\tau)$ is spontaneous magnetization at temperature τ.

The uniaxial anisotropy constant (11) was rewritten as

$$K_u(\tau) = K_v(\tau) - K_d(\tau). \tag{16}$$

We discuss the stability condition of perpendicular remanence (PR) from a balance between the surface and the demagnetization anisotropic energy in the ultrathin film. If $K_u(\tau) > 0$ there is a PR resulting from a perpendicular surface anisotropy strong enough to overcome the shape anisotropy, which is decided by four factors, including the strength of surface anisotropy D, the thicknesss of ultrathin film n, the temperature τ (or σ_ν and Γ_1) and the absolute saturation magnetization $M_s(0)$. Generally, for weak surface anisotropy [11], $\sigma_1 < \sigma_\nu$ ($\nu \neq 1$), and as the temperature increases σ_1 drops more rapidly than σ_ν ($\nu \neq 1$). Hence lower temperature, thinner film, larger D and smaller $M_s(0)$ are advantageous for the presence of PR. As above, we can predict that Fe films and fixed D and $M_s(0)$ have a PR for an intermediate range of film thickness and temperature. For example we interpret that Fe film has a PR just for films less than 5.7 ML. From (14*a*), (15), (16) and $K_u(0) > 0$ we now get the condition for a PR to exist at 0 K:

$$AD(S - 1/2)/n - 2\pi\mu M_s(0) > 0. \tag{17}$$

For ultrathin BCC iron film with $D = 0.8$ meV [5] and $M_s(0) = 1740$ G ($S = 1, \mu S = 2.2\ \mu_B$ and $M_s(0) = \mu S/(a^3/2)$), we obtain $n < 5.7$, which agrees with the result of the experiment [2].

Finally, we can prove that the conditions of $K_u(\tau_r) = 0$ and zero energy gap at the bottom of the spin-wave spectrum are equivalent. From the conditions of zero energy gap

gap given by the appendix, such as $\omega_{01}(\tau_r) = 0$, $\omega_{02}(\tau_r) = 0$, $\omega_{03}(\tau_r) = 0$, $\omega_{04}(\tau_r) = 0$, $\omega_{05}(\tau_r = 0$ (i.e. $c = 0$) and $\omega_{06}(\tau_r) = 0$ (i.e. $c_2 = 0$) for 1, 2, 3, 4, 5 and 6 ML film respectively, we derive their equivalent equations as follows:

$$D\Gamma_1 S\sigma_1 - \mu 4\pi M_s = 0 \qquad \text{(for 1 and 2 ML film)}$$

$$D\Gamma_1 S\sigma_1 - \mu 4\pi M_s = \mu 4\pi M_s \sigma_2/(2\sigma_1) \qquad \text{(for 3 ML film and } 8J_f S\sigma_1 \gg \mu 4\pi M_s)$$

$$D\Gamma_1 S\sigma_1 - \mu 4\pi M_s = \mu 4\pi M_s \sigma_2/\sigma_1 \qquad \text{(for 4 ML film and } 4J_f S\sigma_1 + J_s S\sigma_1 \gg \mu 4\pi M_s)$$

$$2D\Gamma_1 S\sigma_1^2 - (2\sigma_1 + 2\sigma_2 + \sigma_3)\mu 4\pi M_s = 0 \qquad \text{(for 5 ML film and } J_f S\sigma_1 \gg \mu 4\pi M_s)$$

$$D\Gamma_1 S\sigma_1^2 - (\sigma_1 + \sigma_2 + \sigma_3)\mu 4\pi M_s = 0 \qquad \text{(for 6 ML film and } J_f S\sigma_1 \gg \mu 4\pi M_s).$$

From the above equations we now get

$$K_u(\tau_r) = AD\Gamma_1(S\sigma_1)^2/(a^3 n) - 2\pi M_s^2 = \left(AD\Gamma_1 S\sigma_1^2 - \mu 4\pi M_s \sum_\nu \sigma_\nu\right) S/(2\upsilon n) = 0.$$

5. Numerical calculation and discussion

Using a computer to perform the numerical calculation of the temperature dependence of the relative magnetization σ_ν and the Curie temperature T_C, we design the first computer program as follows: Because $\sigma_\nu = 1$ ($\nu = 1, \ldots, n$) at 0 K, if the increment in temperature t and the initial values $\sigma_\nu = 1$ ($\nu = 1, \ldots, n/2$ or $(n+1)/2$) are substituted into (2), (3) and (4*a*)–(4*e*), the final values of $\sigma_\nu \sigma_\nu(t)$ at temperature t are given by iterative solution until $\sum_{\nu=1} \Delta\sigma_\nu(t) < \delta$ (here $\Delta\sigma_\nu(t)$ is the difference between the final value and the final substituting value of $\sigma_\nu(t)$; the value appropriate for δ is 10^{-3} in this paper). Similarly, if the increment in temperature $2t$ and the initial values $\sigma_\nu = \sigma_\nu(t)$ ($\nu = 1, \ldots, n/2$ or $(n+1)/2$) are substituted into (2), (3) and (4*a*)–(4*e*), the final values of $\sigma_\nu = \sigma_\nu(2t)$ at temperature $2t$ are given by iterative solution until $\sum_{\nu=1} \Delta\sigma_\nu(2t) < \delta$ (here $\Delta\sigma_\nu(2t)$ is the difference between the final value and the final substituting value of $\sigma_\nu(2t)$). We repeat the calculation at temperature $3t$, $4t$, ... step by step in the above way until $\sigma_\nu = 0$ ($\nu = 1, 2, \ldots, n$) at the Curie temperature. The relative magnetization σ_ν of each atomic plane as a function of the temperature τ and the Curie temperature τ_C are given. The second computer program to determine the Curie temperature is as follows: Let $\sigma_\nu/\sigma_\mu = (\sigma_\nu/\sigma_1)/(\sigma_\mu/\sigma_1)$; we substitute the initial values of σ_ν/σ_1 ($\nu = 2, 3, \ldots, n/2$ or $(n+1)/2$) into equation (6). By iterative solution until $\sum_{\nu=2} \Delta(\sigma_\nu/\sigma_1) < \epsilon$ (here $\Delta(\sigma_\nu/\sigma_1)$ is the difference between the final value and the final substituting value of σ_ν/σ_1; the value appropriate for ϵ is 10^{-3} in this paper), we obtain the final values of σ_ν/σ_1 and the corresponding value of C_1, which satisfy condition (7). From equation (5) the Curie temperature is determined. After determining the variations of P_1 and σ_ν with τ, the anisotropy constants $K_s(\tau)$, $K_v(\tau)$, $K_d(\tau)$, $K_u(\tau)$ and the energy gap at the bottom of the spin-wave spectrum as functions of the temperature τ can be calculated by (13), (14), (15), (16) and the appendix.

In the following numerical calculation we defined the reduced temperature $\tau = T/T_{Cb}$, where T_{Cb} is the Curie temperature for the bulk magnet and T is absolute temperature; the values appropriate for iron are $S = 1$, $\mu = 2.2\ \mu_B$, $M_s(0) = 1740$ G, $T_{Cb} = 1043$ K, the lattice constant $a = 2.87$ Å, the primitive cell volume $\upsilon = a^3/2$, and the area taken up by one atom in the surface is a^2. First of all, we determine the value of D. From the

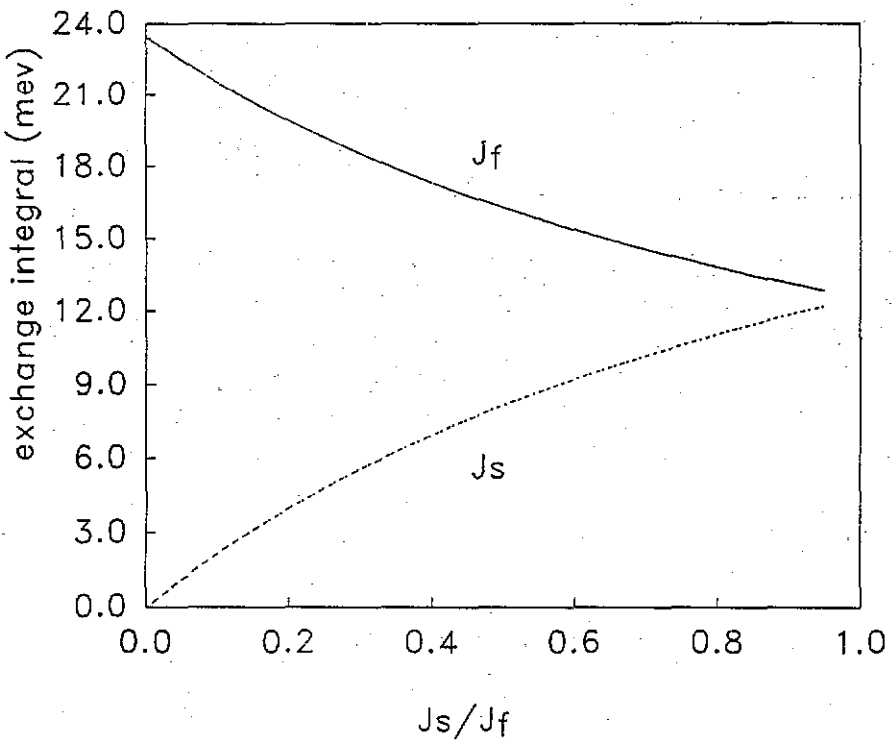

Figure 1. The allowed values of exchange integrals (J_f, J_s) versus J_s/J_f curves for BCC bulk iron with Curie temperature $T_{Cb} = 1043$ K.

data given by Gay *et al* [5] the perpendicular anisotropic surface energy of BCC Fe(001) is 0.4 meV/atom and substituting this value into (13*a*) ($K_s(0) = D/2a^2$, $D/2 = 0.4$ meV), we obtain $D = 0.8$ meV and $K_s(0) = 0.778$ erg cm^{-2}. Secondly, we determine the values of the exchange integrals; in principle, the first- and second-neighbour couplings should be considered. In practice, how to choose the values of the first-neighbour exchange integral J_f and second-neighbour exchange integral J_s was most important. In this paper, the exchange integrals will be regarded as adjustable, to be determined, if possible, from fits to experimental measurements of magnetic properties. If the first- and second-neighbour interactions are considered simultaneously, the bulk Curie temperature T_{Cb} for BCC Fe would depend on both J_f and J_s. According to $T_{Cb} = 1043$ K, using (8) and (8*a*) we determine the allowed values of exchange integrals J_f and J_s (J_f, J_s) for various J_s/J_f. For example, $J_f = 23.47$ meV, $J_s = 0$ (for $J_s/J_f = 0$, $C_b = 1.393$) ..., $J_f = 18.52$ meV, $J_s = 5.554$ meV (for $J_s/J_f = 0.3$, $C_b = 1.099$) and $J_f = 15.03$ meV, $J_s = 9.605$ meV (for $J_s/J_f = 0.639$, $C_b = 0.8921$), respectively, as shown in figure 1. From (5), (6), (7), (5*a*) and (6*a*) we take the value $D = 2$ meV and choose different allowed values of (J_f, J_s), respectively. The calculated results for the Curie temperature as a function of the thickness of the films are about the same in the case of 2 to 6 ML BCC iron films and approximately agree with the experiments [7, 9, 10], as shown in figure 2, where $\tau_C = T_C/T_{Cb}$. Conversely, to choose different allowed values of (J_f, J_s), respectively, the calculated values of the Curie temperature in 1 ML BCC iron films are different and lower than the experimental results ($T_C \simeq 300$ K), as shown in figure 2. Then we could not find a suitable value of J_s to satisfy both 1 ML and 2 to 6 ML, which means that the value of J_s in 1 ML is not equal to the value

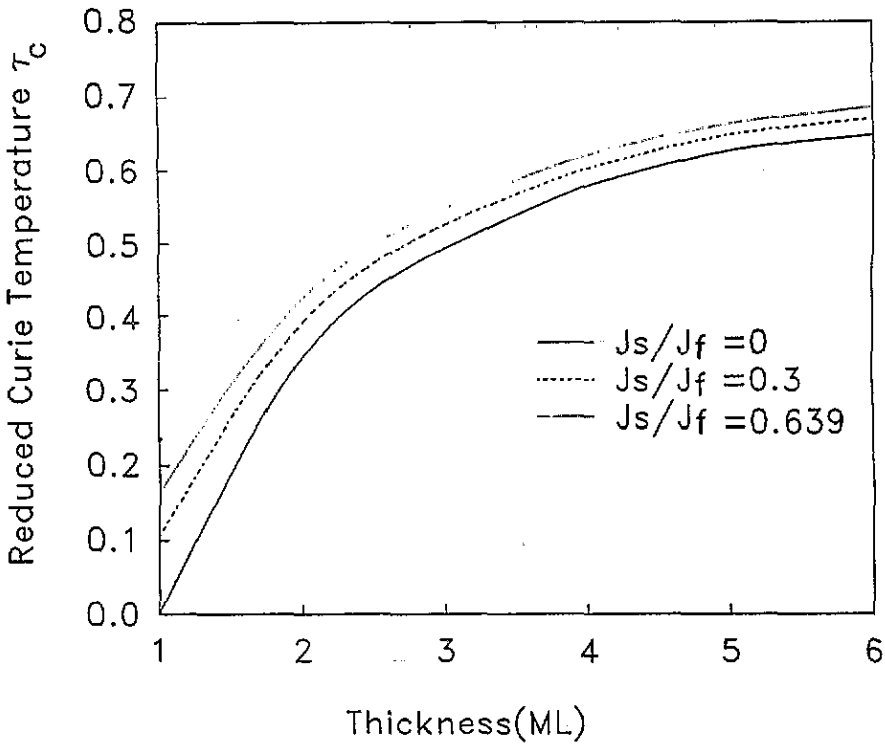

Figure 2. In the case of $D = 2$ meV, the reduced Curie temperature τ_C versus the thickness of n ML films for various (J_f, J_s) or J_s/J_f.

of J_s in 2 to 6 ML. From (5*a*), (6*a*) and letting $D = 0.8$ meV we obtain the Curie temperature T_C as a function of J_s in 1 ML film (see figure 3). If the value for J_s is about 24 meV, it goes beyond the limits of allowed values of J_s; the calculated value of T_C of 1 ML film is 300 K, shown in figures 1 and 3. Therefore we suppose that the exchange integral J_s in 1 ML films should be replaced by J; J is not equal to the allowed values of J_s and can be more than 12.21 meV. The reason is that the exchange interactions of the second-neighbour atoms are enhanced owing to loss of the first-neighbour atoms and great enhancement of the overlap of the electron cloud between the second-neighbour atoms. Furthermore, in accordance with the band theory of ferromagnetism and Ruderman–Kittel–Kasuya–Yoshida (RKKY) indirect exchange mechanism, the effective exchange integral as a function of the interatomic distance R is

$$J(R) = F[\cos(2k_F R) - \sin(2k_F R)/(2k_F R)]/R^3.$$

For iron atom there are 0.6 electrons in the 4s band and the distances of first- and second-neighbour atoms are $0.866a$ and a ($a = 2.87$ Å), respectively. We obtain $k_F = 1.1455 \times 10^{-8}$ cm^{-1} and $J_s/J_f = 0.639$. Therefore in the following numerical calculation for 1 ML films we take the value $J = 23.47$ meV and the values roughly appropriate for 2 ML or more BCC iron film are $J_f = 15.03$ meV, $J_s = 9.605$ meV ($J_s/J_f = 0.639, C_b = 0.8921$). Consider the exchange interaction of second-neighbour atoms. The thoery could explain the fact that there is a rapid change in the T_C values in the monolayer and submonolayer region and a more gradual change for the thicker films [10].

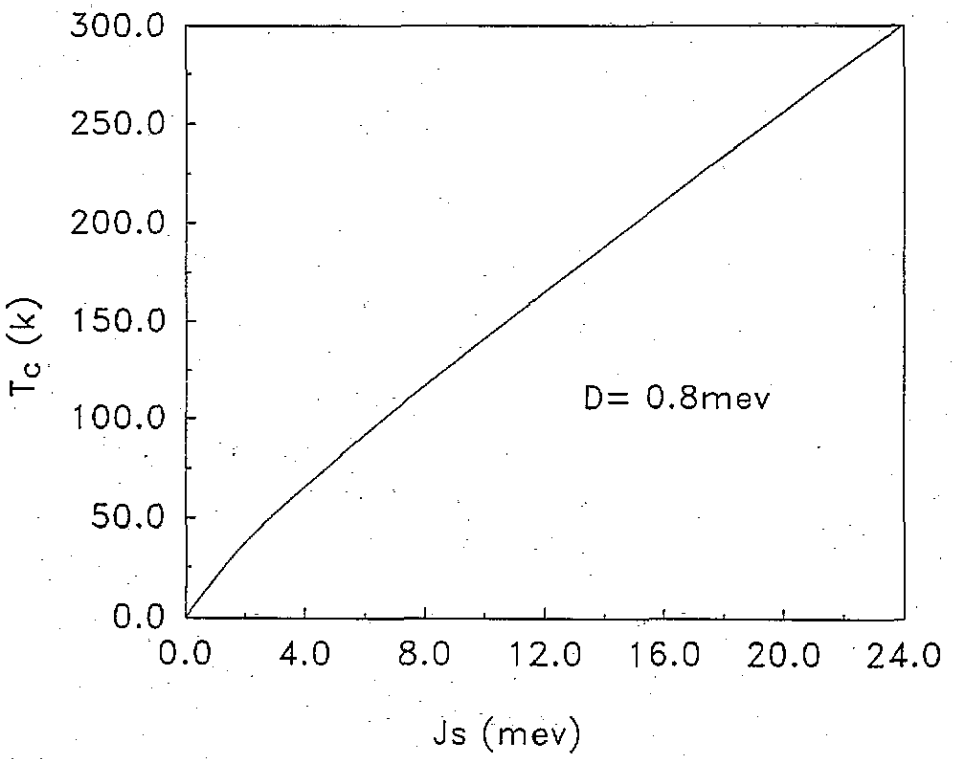

Figure 3. In the case of $D = 0.8$ meV, the Curie temperature T_C versus second-neighbour exchange integral J_s (or J) in 1 ML films.

By employing equations (5), (6), (5*a*) and (6*a*), we perform the numerical calculation of the Curie temperature. In the case of $D = 2$ meV the integrals (6) and (6*a*) can be integrated for 1 ML to 6 ML films, i.e. there is a perpendicular remanence (PR) in the temperature range of 0 K to T_C for 1 to 6 ML films. In the case of $D = 0.95$ meV the integrals (6) and (6*a*) can be integrated for 1, 2, 3 and 4 ML films but no longer for 5 and 6 ML films. This means that there are no PR at least in the range of high temperature for 5 and 6 ML films. In the case of $D = 0.8$ meV the integrals (6) and (6*a*) can be integrated for 1, 2 and 3 ML films but no longer for 4, 5 and 6 ML films. The reduced Curie temperature τ_C versus the thickness of n ML films for various D is illustrated in figure 4, where $\tau_C = T_C/T_{Cb}$. The calculations for the Curie temperature are consistent with the experiments [7, 9, 10].

The variations in $\sigma_v(\tau)$, $\Gamma_1(\tau)$, $K_v(\tau)$, $K_d(\tau)$, ω_{03} and ω_{05} (the energy gap at the bottom of the spin-wave spectrum) with respect to the reduced temperature τ in 3 ML and 5 ML films are illustrated schematically in figures (5*a*) and (*b*), respectively, where $\tau = T/T_{Cb}$, $D = 0.8$ meV. Generally, we can prove that the spontaneous magnetization changes with the position of the atomic planes, which are parallel to the surfaces of n ML films, but the Curie temperatures of atomic planes are all the same. In this paper we have discussed the special case, in which the SA on both surfaces are equal ($D_1 = D_n$), and the spontaneous magnetizations of inequivalent atomic planes are different (see figures 5(*a*) and (*b*)). The surface anisotropy (SA) can be divided into two cases [11]: one is weak SA and the other is strong SA. In the case of weak SA the spontaneous magnetization of the surface atomic plane is less than those of the other atomic planes. If $K_v(\tau_r) - K_d(\tau_r) = 0$ the reversible transition

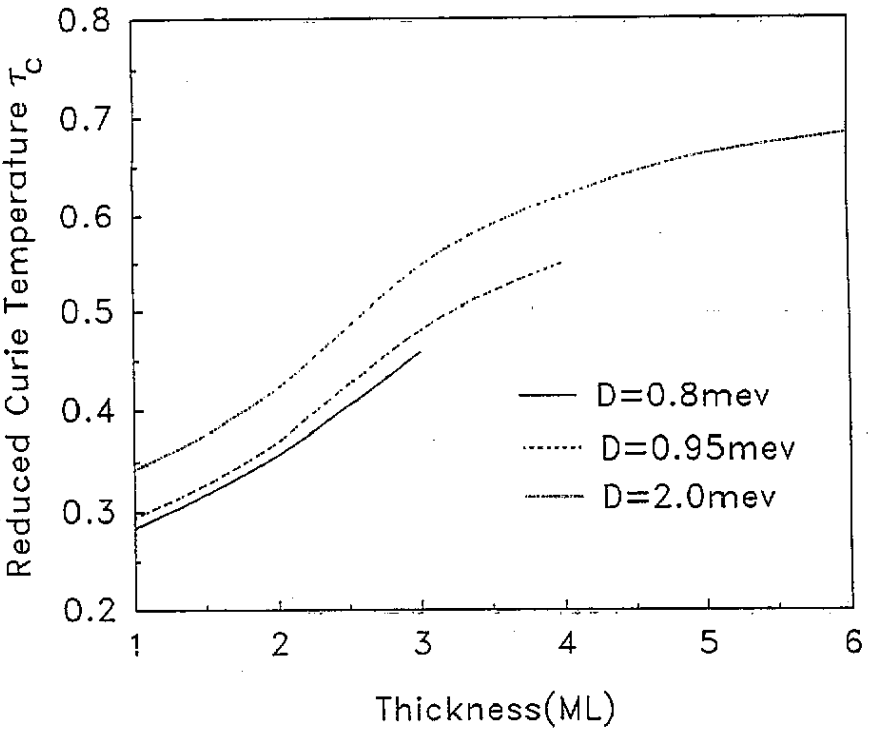

Figure 4. The reduced Curie temperature τ_C versus the thickness of n ML films for various D ($J = 23.47$ meV for 1 ML, $J_f = 15.03$ meV and $J_s = 9.605$ meV for 2 ML or more film).

beween perpendicular (at low temperature $\tau < \tau_r$) and in-plane (at high temperature $\tau > \tau_r$) magnetization in ultrathin films will happen at temperature τ_r. In the case of strong SA the strong spontaneous magnetization of the surface atomic plane is more than those of the other atomic planes. If $K_v(\tau_r) - K_d(\tau_r) = 0$ at temperature τ_r there is a reversible transition between in-plane (at low temperature $\tau < \tau_r$) and perpendicular (at high temperature $\tau > \tau_r$) magnetization in ultrathin films. Generally, the energy gaps at the bottom of spin-wave spectra in monolayer and submonolayer Fe films have the maximum values possible at absolute zero degrees. Then, as the temperature is raised (or σ_v decreased), their magnitudes decrease monotonically until $\sigma_v = 0$; they become zero at the Curie temperature, as ω_{03} shown in figure 5(a). However, if the ultrathin films have a reversible transition between perpendicular and in-plane magnetization ($\sigma_v \neq 0$) at temperature τ_r, the calculated results have proved that the zero energy gap at the bottom of the spin-wave spectrum and the zero uniaxial anisotropy constant would happen simultaneously at the same temperature τ_r. For example, in the case $D = 0.8$ meV for 5 ML film when the temperature has gone up to $\tau = \tau_r = 0.21$, the film has $\omega_{05}(\tau_r) = 0$ and $K_v(\tau_r) - K_d(\tau_r) = 0$ accompanied by discontinuity changes in the spontaneous magnetization $\sigma_v(\tau_r)$ at the same temperature τ_r, as shown in figure 5(b). From (4c) we get $\Gamma_1(0) = 1$ at 0 K and $\Gamma_1(\tau_c) = 0.75$ at T_C. $\Gamma_1(\tau)$ as a function of temperature in 3 ML and 5 ML films has been shown in figures 5(a) and (b).

In the case of $D = 0.8$ meV, which was established by Gay [5] (0.4 meV/atom), the surface anisotropy constant $K_s(0)$ equals 0.778 erg cm^{-2} at 0 K. From (2), (3) and (13) we further give the variation in the surface anisotropy constant $K_s(\tau)$ of n ML film with respect

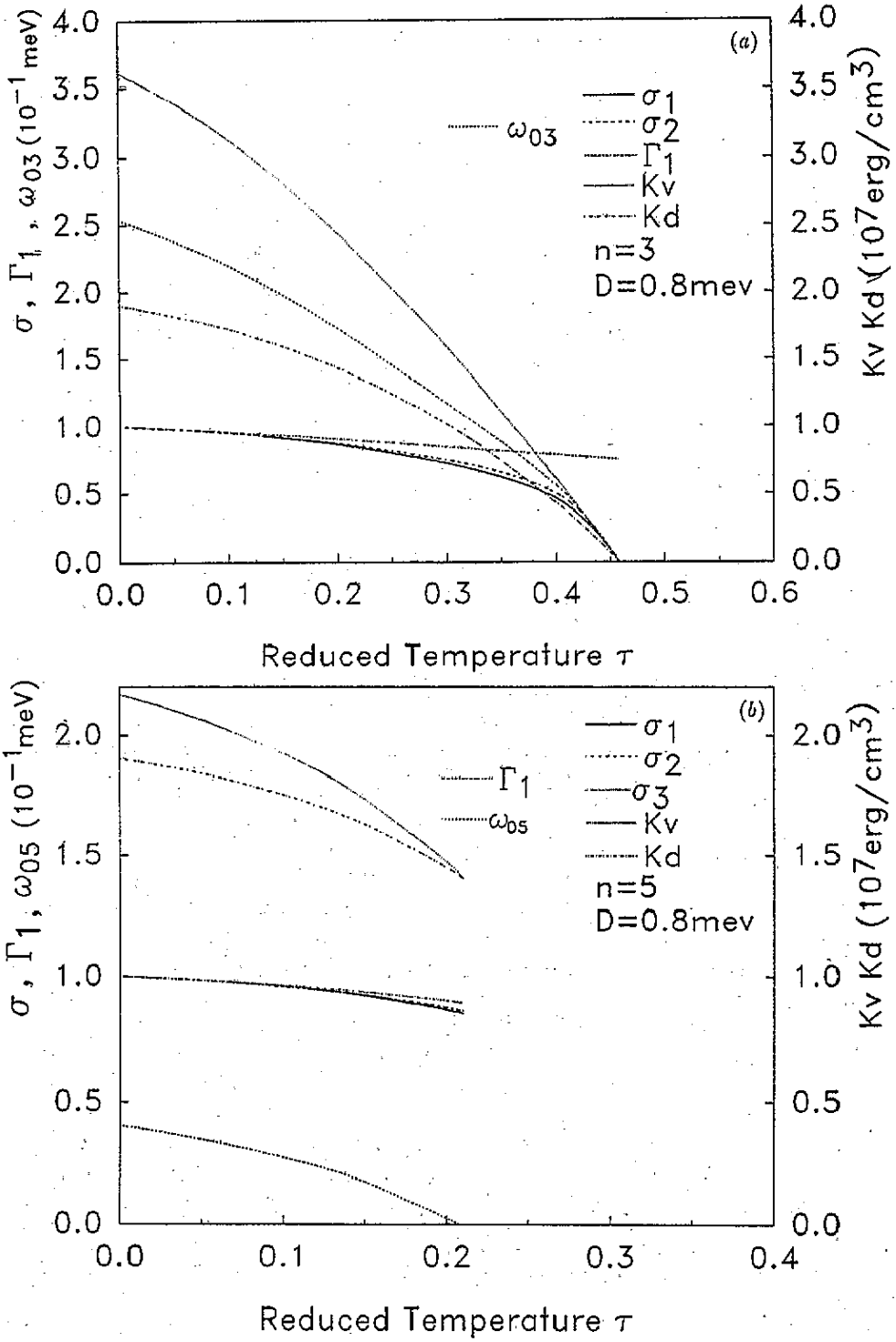

Figure 5. Curves of the relative magnetization of atomic planes σ_v, the effective volume anisotropy constant K_v, the shape anisotropy constant K_d, the energy gap at the bottom of the spin-wave spectrum $\omega_{03}(a)$ and $\omega_{05}(b)$ and Γ_1 as functions of reduced temperature τ for $D = 0.8$ meV, $J_f = 15.03$ meV and $J_s = 9.605$ meV in (a) 3 ML film and (b) 5 ML film.

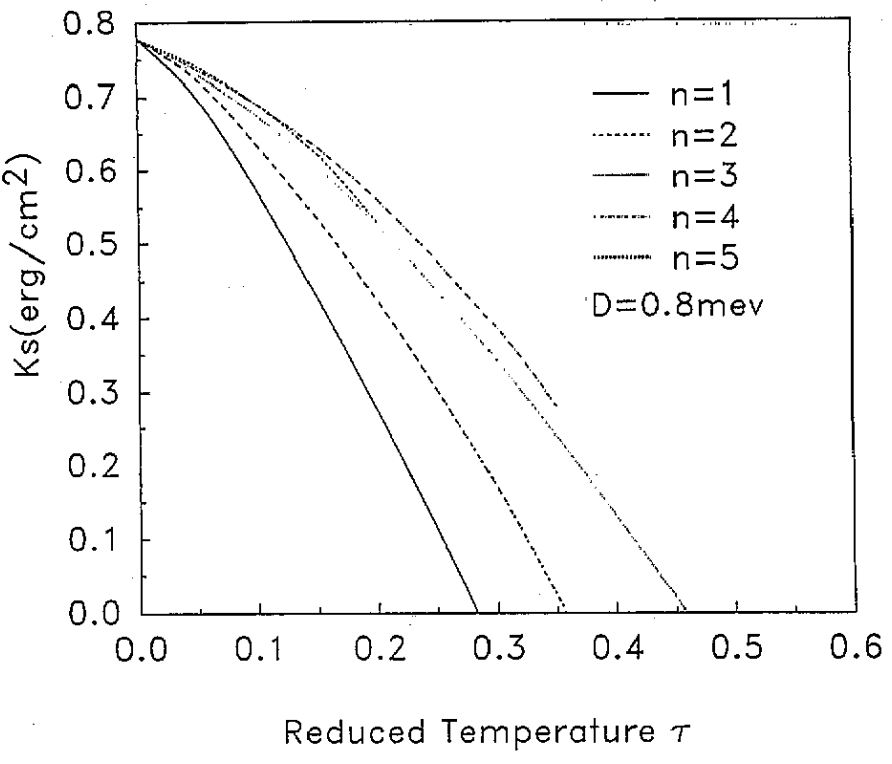

Figure 6. The surface anisotropy constant K_s as a function of reduced temperature τ for $D = 0.8$ meV in n ML films ($J = 23.47$ meV for 1 ML, $J_f = 15.03$ meV and $J_s = 9.605$ meV for 2 ML or more film).

to the reduced temperature τ, shown in figure 6, where $\tau = T/T_{Cb}$. The integral (3) for 6 ML film cannot be integrated in the whole range of temperature, while the integrals (3) for 5 and 4 ML films cannot be integrated in the range of reduced temperature, higher than 0.21 and 0.38, respectively. The curve $(K_s - \tau)$ is a reflection of the temperature dependence of the stabilization of PR.

From (2), (3), (14), (15) and (16) we can calculate the uniaxial anisotropy constant $K_u(\tau)$ as a function of the reduced temperature τ for various D in 1 to 6 ML films; D takes the values $D = 0.7$, 0.8, 0.95 and 2 meV, respectively. Various $(K_u - \tau)$ curves are illustrated schematically in figures 7–10 where $\tau = T/T_{Cb}$. For the case of $D = 0.7$ meV corresponding to $K_s(0) = 0.681$ erg cm^{-2}, as shown in figure 7, the integrals (3*a*), (6*a*) for 1 ML film and (3), (6) for 2 and 3 ML films can be integrated in the whole range of temperature. The integral (3) for 4 ML film can be integrated in 0 to 0.28 range of reduced temperature and cannot be integrated at reduced temperature higher than 0.28. The integrals (3) for 5 and 6 ML films cannot be integrated in the whole range of temperature; i.e. 1,2 and 3 ML films have $K_u(\tau) > 0$ and a PR in 0 K to T_C range, while 4 ML films have $K_u(\tau) > 0$ in 0 to 0.28 range of reduced temperature and $K_u(\tau_r) = 0$ at magnetization transition point $\tau_r = 0.28$. There are no PR in 5 and 6 ML films. Figure 8 shows that in the case of $D = 0.8$ meV corresponding to $K_s(0) = 0.778$ erg cm^{-2}, 1, 2 and 3 ML films have a PR in 0 K to T_C range, 4 and 5 ML films have the transition between perpendicular and in-plane magnetization at transition point $\tau_r = 0.38$ and $\tau_r = 0.21$ respectively, and there

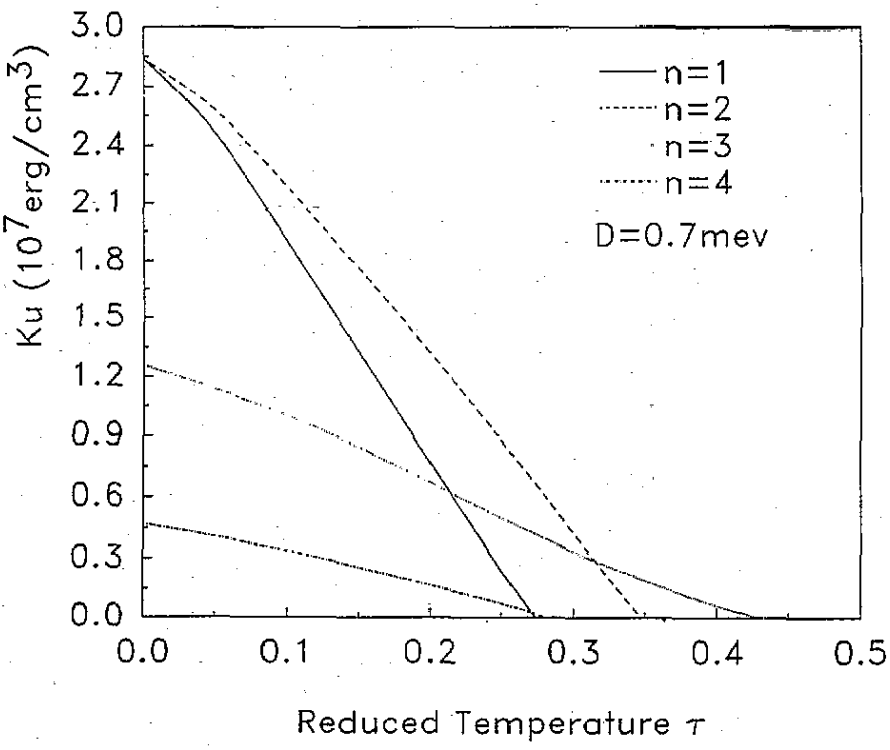

Figure 7. In the case of $D = 0.7$ meV, the uniaxial anisotropy constant K_u of n ML films as a function of the reduced temperature τ ($J = 23.47$ meV for 1 ML, $J_f = 15.03$ meV and $J_s = 9.605$ meV for 2 ML or more film).

are no PR in 6 ML film. Figure 9 shows that in the case of $D = 0.95$ meV corresponding to $K_s(0) = 0.924$ erg cm^{-2}, 1, 2, 4 and 4 ML films have a PR in 0 K to T_C range, while 5 and 6 ML films have the transition between perpendicular and in-plane magnetization at $\tau_r = 0.36$ and $\tau_r = 0.21$ respectively. Figure 10 shows that in the case of $D = 2$ meV corresponding to $K_s(0) = 1.95$ erg cm^{-2} the films of 6 ML or thinner BCC Fe have a PR in 0 K to T_C range. Comparing figures 7–10 we find that the SA and the thickness of ultrathin film sensitively affect the nature of PR. It has been shown that, in the case of weak SA [11], lower temperature, thinner film and larger D are advantageous for the presence of PR. If $D < 0.4$ meV there is no PR for any Fe film thickness. In the case of fixed D, as the thickness of ultrathin Fe film is decreased, the transition point τ_r rises. By employing the above-mentioned theory, we can interpret the experimental results. For example, the experiments reported by [1] and [2] can be interpreted by the case of $D \simeq 0.8$ meV (shown in figure 8), while the experiment reported by [3] may be explained by the discrepancy of surface situation (leads to different values of D) of the films. We suppose that SA is extremely sensitive to lattice geometry, type of substrate and coating layers, adsorbates, lattice imperfections and stress and strain due to growth conditions. Owing to the strong dependence of SA on the actual film preparation, different experimental results have been obtained for the same system (for example, Fe/Ag(001)).

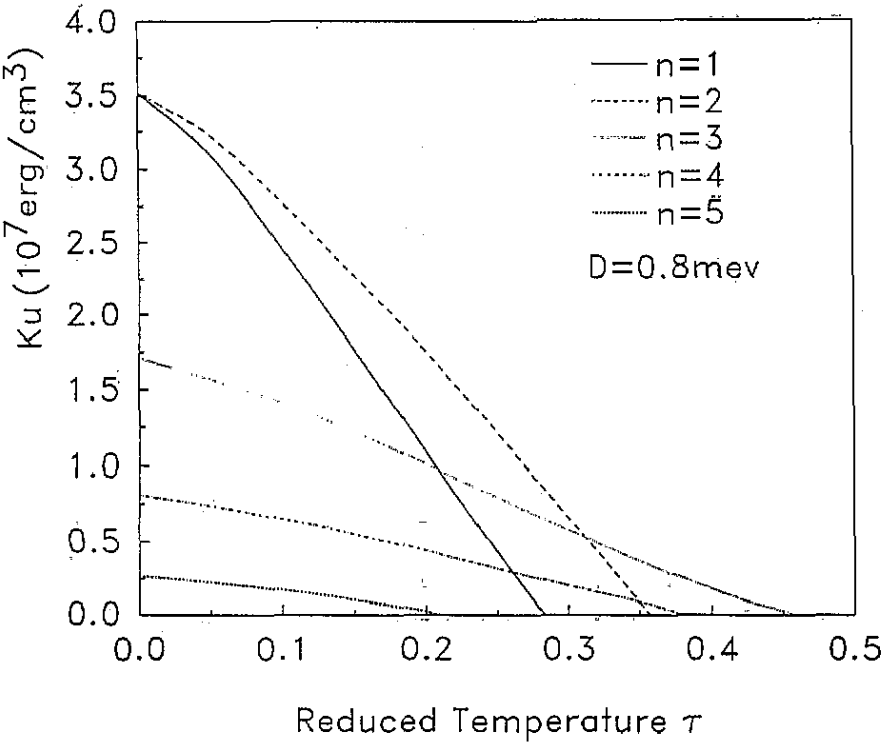

Figure 8. In the case of $D = 0.8$ meV, the uniaxial anisotropy constant K_u of n ML films as a function of the reduced temperature τ ($J = 23.47$ meV for 1 ML, $J_f = 15.03$ meV and $J_s = 9.605$ meV for 2 ML or more film).

6. Conclusion

The dependence of Curie temperature and PR on the thickness of ultrathin films results from perpendicular surface anisotropy in the films, while the reversible transition between perpendicular and in-plane magnetization is attributed to the temperature dependence of the perpendicular surface anisotropy constant. For ultrathin BCC iron film with perpendicular anisotropic surface energy 0.4 meV/atom ($D \doteq 0.8$ meV) there is a PR in 0 K to T_C range for 1, 2 and 3 ML films, a reversible transition between perpendicular and in-plane magnetization in 4 and 5 ML films (as the thickness of ultrathin film is decreased, the transition point τ_r rises) and no PR in 6 ML film. We introduce the SA to describe the surface situation of ultrathin films. Theory has shown that the discrepancies of SA in an ultrathin film strongly change the behaviours of ferromagnetic phase transition and PR. Thus, the observed discrepancies beween various experiments could be explained by the discrepancies of SA of various experimental specimens.

In this work, the formulae for F_k and the anisotropy constants $K_s(T)$ and $K_v(T)$ resulting from surface single-ion anisotropy of ultrathin film have been derived for the first time. By employing the expressions for $K_v(T)$ and $K_d(T)$ given in the present paper, we discuss the stability condition of PR from a balance between surface and demagnetization anisotropy energy in the ultrathin film. The theory explains many observed phenomena.

If the exchange integrals are regarded as adjustable from fits to experimental measurements of magnetic properties, by using either the first-neighbour exchange

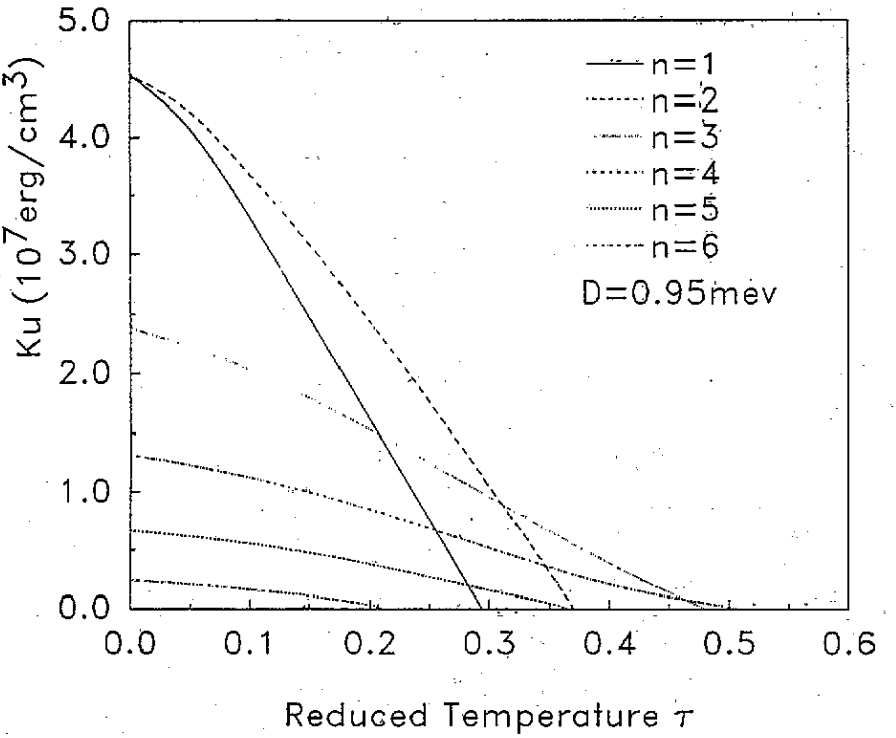

Figure 9. In the case of $D = 0.95$ meV, the uniaxial anisotropy constant K_u of n ML films as a function of the reduced temperature τ ($J = 23.47$ meV for 1 ML, $J_f = 15.03$ meV and $J_s = 9.605$ meV for 2 ML or more film).

interaction approximation or to take into account the second-neighbour interaction, the calculated results for anisotropy constants, PR and transition point in 2 ML or more BCC Fe films are not changed. In order to interpret the experiments we expect that the second-neighbour exchange interaction was enhanced markedly in 1 ML BCC Fe film.

Acknowledgments

I am greatly indebted to Mr Ying Xiang who has assisted in the preparation of the figures. The research is supported by the Natural Science Foundation of China under Grant No 1880767.

Appendix

For the case $n = 1$ (ν and $k = 1$)

$$\omega_{h1} = \omega_{h1} \qquad \text{(see equation (6}a\text{))}$$
$$U_{11}^2 = 1$$

and ω_{01} is the energy gap at the bottom of the spin-wave spectrum.

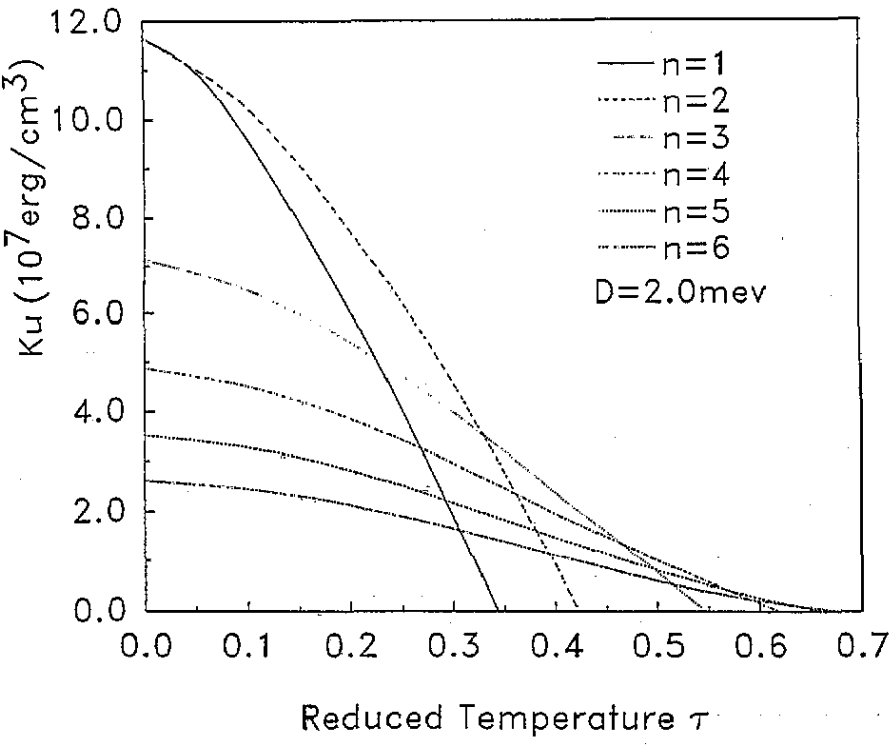

Figure 10. In the case of $D = 2$ meV, the uniaxial anisotropy constant K_u of n ML films as a function of the reduced temperature τ ($J = 23.47$ meV for 1 ML, $J_f = 15.03$ meV and $J_s = 9.605$ meV for 2 ML or more film).

For the case $n = 2$ (ν and $k = 1, 2$; $\sigma_2 = \sigma_1$)

$$\omega_{h1} = E_1 + J_1 \qquad \omega_{h2} = E_1 - J_1$$
$$U_{11}^2 = U_{12}^2 = \tfrac{1}{2}$$

and ω_{02} is the energy gap at the bottom of the spin-wave spectrum.

For the case $n = 3$ (ν and $k = 1, 2, 3$; $\sigma_3 = \sigma_1$)

$$\omega_{h1} = E_1 + J_1' \qquad \omega_{h2} = \tfrac{1}{2}(A + B) \qquad \omega_{h3} = \tfrac{1}{2}(A - B)$$
$$U_{11}^2 = \tfrac{1}{2} \qquad U_{12}^2 = \tfrac{1}{4}(1 + C/B) \qquad U_{13}^2 = \tfrac{1}{4}(1 - C/B)$$
$$U_{21}^2 = 0 \qquad U_{22}^2 = \tfrac{1}{2}(1 - C/B) \qquad U_{23}^2 = \tfrac{1}{2}(1 + C/B)$$
$$A = E_1 + E_2 - J_1' \qquad C = E_1 - E_2 - J_1' \qquad B = (C^2 + 8J_1J_2)^{1/2}$$

and ω_{03} is the energy gap at the bottom of the spin-wave spectrum.

For the case $n = 4$ (ν and $k = 1, 2, 3, 4$; $\sigma_1 = \sigma_4$; $\sigma_2 = \sigma_3$)

$$\omega_{h1} = \tfrac{1}{2}(A + E) \qquad \omega_{h2} = \tfrac{1}{2}(A - E) \qquad \omega_{h3} = \tfrac{1}{2}(B + F) \qquad \omega_{h4} = \tfrac{1}{2}(B - F)$$
$$U_{11}^2 = \tfrac{1}{4}(1+D/E) \qquad U_{12}^2 = \tfrac{1}{4}(1-D/E) \qquad U_{13}^2 = \tfrac{1}{4}(1+C/F) \qquad U_{14}^2 = \tfrac{1}{4}(1-C/F)$$

$$U_{21}^2 = \tfrac{1}{4}(1-D/E) \qquad U_{22}^2 = \tfrac{1}{4}(1+D/E) \qquad U_{23}^2 = \tfrac{1}{4}(1-C/F) \qquad U_{24}^2 = \tfrac{1}{4}(1+C/F)$$

$$A = E_1 + E_2 + J_2 \qquad B = E_1 + E_2 - J_2 \qquad C = E_1 - E_2 + J_2 \qquad D = E_1 - E_2 - J_2$$

$$E = [(E_1 - E_2 - J_2)^2 + 4(J_1 - J_1')(J_2 - J_2')]^{1/2}$$

$$F = [(E_1 - E_2 + J_2)^2 + 4(J_1 + J_1')(J_2 + J_2')]^{1/2}$$

and ω_{04} is the energy gap at the bottom of the spin-wave spectrum.

For the case $n = 5$ (ν and $k = 1, 2, 3, 4, 5$; $\sigma_1 = \sigma_5$; $\sigma_2 = \sigma_4$), from the factorization of equation (4), we get the characteristic equations

$$(\omega_{hk} - E_1)(\omega_{hk} - E_2 - J_2') - J_1 J_2 = 0 \tag{A1}$$

$$(\omega_{hk} - E_1)(\omega_{hk} - E_2 + J_2')(\omega_{hk} - E_3) - J_1 J_2(\omega_{hk} - E_3) - 2J_2 J_3(\omega_{hk} - E_1) - 2J_1' J_3'(\omega - E_2 + J_2') + 2J_2(J_1 J_3' + J_1' J_3) = 0. \tag{A2}$$

We determine ω_{h1}, ω_{h2} from (A1) and $\omega_{h3}, \omega_{h4}, \omega_{h5}$ from (A2):

$$\omega_{h1} = (E_1 + E_2 + J_2' + Q)/2 \qquad \omega_{h2} = (E_1 + E_2 + J_2' - Q)/2$$

$$\omega_{h3} = R\cos[(\theta - 2\pi)/3] - a \qquad \omega_{h4} = R\cos(\theta/3) - a \qquad \omega_{h5} = R\cos[(\theta + 2\pi)/3] - a$$

where

$$Q = [(E_1 - E_2 - J_2')^2 + 4J_1 J_2]^{1/2} \qquad a = -(E_1 + E_2 - J_2' + E_3)/3$$

$$b = (E_2 - J_2')(E_1 + E_3) + E_1 E_3 - (J_1 J_2 + 2J_2 J_3 + 2J_1' J_3')$$

$$c = E_3[J_1 J_2 - E_1(E_2 - J_2')] + 2E_1 J_2 J_3 + 2(E_2 - J_2')J_1' J_3' + 2J_2(J_1 J_3' + J_1' J_3)$$

$$U = -c/2 - a(a^2 - b/2) \qquad P = b/3 - a^2$$

$$V = (|U^2 + P^3|)^{1/2} \qquad \text{(because of } U^2 + P^3 < 0\text{)}$$

$$\theta = \tan^{-1}(V/U) \qquad R = 2(U^2 + V^2)^{1/6}.$$

From equations (A1) and (A2), we can simplify $U_{\nu k}^2$ as follows

$$U_{11}^2 = \frac{\omega_{h1} - E_2 - J_2'}{2(\omega_{h1} - \omega_{h2})} \qquad U_{12}^2 = \frac{\omega_{h2} - E_2 - J_2'}{2(\omega_{h2} - \omega_{h1})}$$

$$U_{13}^2 = \frac{(\omega_{h3} - E_2 + J_2')(\omega_{h3} - E_3) - 2J_2 J_3}{2(\omega_{h3} - \omega_{h4})(\omega_{h3} - \omega_{h5})}$$

$$U_{14}^2 = \frac{(\omega_{h4} - E_2 + J_2')(\omega_{h4} - E_3) - 2J_2 J_3}{2(\omega_{h4} - \omega_{h3})(\omega_{h4} - \omega_{h5})}$$

$$U_{15}^2 = \frac{(\omega_{h5} - E_2 + J_2')(\omega_{h5} - E_3) - 2J_2 J_3}{2(\omega_{h5} - \omega_{h3})(\omega_{h5} - \omega_{h4})} \qquad U_{21}^2 = \frac{\omega_{h1} - E_1}{2(\omega_{h1} - \omega_{h2})}$$

$$U_{22}^2 = \frac{\omega_{h2} - E_1}{2(\omega_{h2} - \omega_{h1})} \qquad U_{23}^2 = \frac{(\omega_{h3} - E_1)(\omega_{h3} - E_3) - 2J_1' J_3'}{2(\omega_{h3} - \omega_{h4})(\omega_{h3} - \omega_{h5})}$$

$$U_{24}^2 = \frac{(\omega_{h4} - E_1)(\omega_{h4} - E_3) - 2J_1'J_3'}{2(\omega_{h4} - \omega_{h3})(\omega_{h4} - \omega_{h5})} \qquad U_{25}^2 = \frac{(\omega_{h5} - E_1)(\omega_{h5} - E_3) - 2J_1'J_3'}{2(\omega_{h5} - \omega_{h3})(\omega_{h5} - \omega_{h4})}$$

$$U_{31}^2 = 0 \qquad U_{32}^2 = 0 \qquad U_{33}^2 = \frac{(\omega_{h3} - E_1)(\omega_{h3} - E_2 + J_2') - J_1J_2}{(\omega_{h3} - \omega_{h4})(\omega_{h3} - \omega_{h5})}$$

$$U_{34}^2 = \frac{(\omega_{h4} - E_1)(\omega_{h4} - E_2 + J_2') - J_1J_2}{(\omega_{h4} - \omega_{h3})(\omega_{h4} - \omega_{h5})} \qquad U_{35}^2 = \frac{(\omega_{h5} - E_1)(\omega_{h5} - E_2 + J_2') - J_1J_2}{(\omega_{h5} - \omega_{h3})(\omega_{h5} - \omega_{h4})}$$

and ω_{05} is the energy gap at the bottom of the spin-wave spectrum.

For the case $n = 6$ (ν and $k = 1, 2, 3, 4, 5, 6$; $\sigma_1 = \sigma_6$; $\sigma_2 = \sigma_5$; $\sigma_3 = \sigma_4$), from the factorization of equation (4), we get the characteristic equations

$$\begin{aligned}(\omega_{hk} - E_1)(\omega_{hk} - E_2)(\omega_{hk} - E_3 - J_3) - J_1J_2(\omega_{hk} - E_3 - J_3) \\ - (J_2J_3 - J_2J_3' - J_2'J_3 + J_2'J_3')(\omega_{hk} - E_1) - J_1'J_3'(\omega_{hk} - E_2) \\ + J_2(J_1J_3' + J_1'J_3) - J_3'(J_1J_2' + J_1'J_2) = 0\end{aligned} \tag{A3}$$

$$\begin{aligned}(\omega_{hk} - E_1)(\omega_{hk} - E_2)(\omega_{hk} - E_3 + J_3) - J_1J_2(\omega_{hk} - E_3 + J_3) \\ - (J_2J_3 + J_2J_3' + J_2'J_3 + J_2'J_3')(\omega_{hk} - E_1) \\ - J_1'J_3'(\omega_{hk} - E_2) + J_2(J_1J_3' + J_1'J_3) + J_3'(J_1J_2' + J_1'J_2) = 0.\end{aligned} \tag{A4}$$

We determine ω_{h1}, ω_{h2}, ω_{h3} from (A3) and ω_{h4}, ω_{h5}, ω_{h6} from (A4):

$$\omega_{h1} = R_1\cos[(\theta_1 - 2\pi)/3] - a_1 \qquad \omega_{h2} = R_1\cos(\theta_1/3) - a_1$$

$$\omega_{h3} = R_1\cos[(\theta_1 + 2\pi)/3] - a_1 \qquad \omega_{h4} = R_2\cos[(\theta_2 - 2\pi)/3] - a_2$$

$$\omega_{h5} = R_2\cos(\theta_2/3) - a_2 \qquad \omega_{h6} = R_2\cos[(\theta_2 + 2\pi)/3] - a_2$$

where

$$a_1 = -(E_1 + E_2 + E_3 + J_3)/3$$

$$b_1 = E_1E_2 + (E_1 + E_2)(E_3 + J_3) - J_2(J_1 + J_3) + (J_2J_3' + J_2'J_3) - J_3'(J_1' + J_2')$$

$$\begin{aligned}c_1 = -(E_1E_2 - J_1J_2)(E_3 + J_3) + E_1(J_2J_3 + J_2'J_3' - J_2J_3' - J_2'J_3) + E_2J_1'J_3' \\ + J_2(J_1J_3' + J_1'J_3) - J_3'(J_1J_2' + J_1'J_2)\end{aligned}$$

$$U_1 = -c_1/2 - a_1(a_1^2 - b_1/2)$$

$$P_1 = b_1/3 - a_1^2 \qquad V_1 = (|U_1^2 + P_1^3|)^{1/2} \qquad \text{(because of } U_1^2 + P_1^3 < 0\text{)}$$

$$\theta_1 = \tan^{-1}(V_1/U_1) \qquad R_1 = 2(U_1^2 + V_1^2)^{1/6}$$

$$a_2 = -(E_1 + E_2 + E_3 - J_3)/3$$

$$b_2 = E_1E_2 + (E_1 + E_2)(E_3 - J_3) - J_2(J_1 + J_3) - (J_2J_3' + J_2'J_3) - J_3'(J_1' + J_2')$$

$$\begin{aligned}c_2 = -(E_1E_2 - J_1J_2)(E_3 - J_3) + E_1(J_2J_3 + J_2'J_3' + J_2J_3' + J_2'J_3) + E_2J_1'J_3' \\ + J_2(J_1J_3' + J_1'J_3) + J_3'(J_1J_2' + J_1'J_2)\end{aligned}$$

$$U_2 = -c_2/2 - a_2(a_2^2 - b_2/2)$$

$$P_2 = b_2/3 - a_2^2 \qquad V_2 = (|U_2^2 + P_2^3|)^{1/2} \qquad \text{(because of } U_2^2 + P_2^3 < 0\text{)}$$

$$\theta_2 = \tan^{-1}(V_2/U_2) \qquad R_2 = 2(U_2^2 + V_2^2)^{1/6}.$$

From equations (A3) and (A4), we can simplify $U^2_{\nu k}$ as follows

$$U^2_{11} = \frac{(\omega_{h1} - E_2)(\omega_{h1} - E_3 - J_3) - J_2 J_3 - J_2' J_3' + J_2 J_3' + J_2' J_3}{2(\omega_{h1} - \omega_{h2})(\omega_{h1} - \omega_{h3})}$$

$$U^2_{12} = \frac{(\omega_{h2} - E_2)(\omega_{h2} - E_3 - J_3) - J_2 J_3 - J_2' J_3' + J_2 J_3' + J_2' J_3}{2(\omega_{h2} - \omega_{h3})(\omega_{h2} - \omega_{h1})}$$

$$U^2_{13} = \frac{(\omega_{h3} - E_2)(\omega_{h3} - E_3 - J_3) - J_2 J_3 - J_2' J_3' + J_2 J_3' + J_2' J_3}{2(\omega_{h3} - \omega_{h1})(\omega_{h3} - \omega_{h2})}$$

$$U^2_{14} = \frac{(\omega_{h4} - E_2)(\omega_{h4} - E_3 + J_3) - J_2 J_3 - J_2' J_3' - J_2 J_3' - J_2' J_3}{2(\omega_{h4} - \omega_{h5})(\omega_{h4} - \omega_{h6})}$$

$$U^2_{15} = \frac{(\omega_{h5} - E_2)(\omega_{h5} - E_3 + J_3) - J_2 J_3 - J_2' J_3' - J_2 J_3' - J_2' J_3}{2(\omega_{h5} - \omega_{h6})(\omega_{h5} - \omega_{h4})}$$

$$U^2_{16} = \frac{(\omega_{h6} - E_2)(\omega_{h6} - E_3 + J_3) - J_2 J_3 - J_2' J_3' - J_2 J_3' - J_2' J_3}{2(\omega_{h6} - \omega_{h4})(\omega_{h6} - \omega_{h5})}$$

$$U^2_{21} = \frac{(\omega_{h1} - E_1)(\omega_{h1} - E_3 - J_3) - J_1' J_3'}{2(\omega_{h1} - \omega_{h2})(\omega_{h1} - \omega_{h3})}$$

$$U^2_{22} = \frac{(\omega_{h2} - E_1)(\omega_{h2} - E_3 - J_3) - J_1' J_3'}{2(\omega_{h2} - \omega_{h3})(\omega_{h2} - \omega_{h1})}$$

$$U^2_{23} = \frac{(\omega_{h3} - E_1)(\omega_{h3} - E_3 - J_3) - J_1' J_3'}{2(\omega_{h3} - \omega_{h1})(\omega_{h3} - \omega_{h2})}$$

$$U^2_{24} = \frac{(\omega_{h4} - E_1)(\omega_{h4} - E_3 + J_3) - J_1' J_3'}{2(\omega_{h4} - \omega_{h5})(\omega_{h4} - \omega_{h6})}$$

$$U^2_{25} = \frac{(\omega_{h5} - E_1)(\omega_{h5} - E_3 + J_3) - J_1' J_3'}{2(\omega_{h5} - \omega_{h6})(\omega_{h5} - \omega_{h4})}$$

$$U^2_{26} = \frac{(\omega_{h6} - E_1)(\omega_{h6} - E_3 + J_3) - J_1' J_3'}{2(\omega_{h6} - \omega_{h4})(\omega_{h6} - \omega_{h5})}$$

$$U^2_{31} = \frac{(\omega_{h1} - E_1)(\omega_{h1} - E_2) - J_1 J_2}{2(\omega_{h1} - \omega_{h2})(\omega_{h1} - \omega_{h3})} \qquad U^2_{32} = \frac{(\omega_{h2} - E_1)(\omega_{h2} - E_2) - J_1 J_2}{2(\omega_{h2} - \omega_{h3})(\omega_{h2} - \omega_{h1})}$$

$$U^2_{33} = \frac{(\omega_{h3} - E_1)(\omega_{h3} - E_2) - J_1 J_2}{2(\omega_{h3} - \omega_{h1})(\omega_{h3} - \omega_{h2})} \qquad U^2_{34} = \frac{(\omega_{h4} - E_1)(\omega_{h4} - E_2) - J_1 J_2}{2(\omega_{h4} - \omega_{h5})(\omega_{h4} - \omega_{h6})}$$

$$U^2_{35} = \frac{(\omega_{h5} - E_1)(\omega_{h5} - E_2) - J_1 J_2}{2(\omega_{h5} - \omega_{h6})(\omega_{h5} - \omega_{h4})} \qquad U^2_{36} = \frac{(\omega_{h6} - E_1)(\omega_{h6} - E_2) - J_1 J_2}{2(\omega_{h6} - \omega_{h4})(\omega_{h6} - \omega_{h5})}$$

and ω_{06} is the energy gap at the bottom of the spin-wave spectrum.

References

[1] Jonker B T, Walker K H, Kisker E, Prinz G A and Carbone C 1986 *Phys. Rev. Lett.* **57** 142
[2] Koon N C, Jonker B T, Volkening F A, Krebs J J and Prinz G A 1987 *Phys. Rev. Lett.* **59** 2463
[3] Stampanoni M, Vaterlaus A, Aeschlimann M and Meier F 1987 *Phys. Rev. Lett.* **59** 2483
[4] Cabanel R, Etienne P, Lequien S, Creuzet G, Barthelemy A and Fert A 1990 *J. Appl. Phys.* **67** 5409
[5] Gay J G and Richter R 1987 *J. Appl. Phys.* **61** 3362
[6] Pappas D P, Kamper K P, Miller B P, Hopster H, Fowler D E, Luntz A C, Brundle C R and Shen Z X 1991 *J. Appl. Phys.* **69** 5209
[7] Rau C, Jin C and Xing G 1990 *Phys. Lett.* **114** 406
[8] Gradmann U 1974 *Appl. Phys.* **3** 161
[9] Durr W, Taborelli M, Paul O, Germar R, Gudat W, Pescia D and Landolt M 1989 *Phys. Rev. Lett.* **62** 206
[10] Liu C and Bader S D 1990 *J. Appl. Phys.* **67** 5758
Liu C, Mong E R and Bader S D 1988 *Phys. Rev. Lett.* **69** 2422
[11] Shi L P and Yang W G 1992 *J. Phys.: Condens. Matter* **4** 7997
[12] Shi L P, Ji Z R and Hu L 1991 *J. Appl. Phys.* **69** 5313
[13] Yafet Y and Gyorgy E M 1988 *Phys. Rev.* B **38** 9145
[14] Anderson F B and Callen H B 1964 *Phys. Rev.* **136** A1068
[15] Lines M E 1967 *Phys. Rev.* **156** 534
[16] Devlin J F 1971 *Phys. Rev.* B **4** 136
[17] Endo Y and Ayukawa T 1989 *J. Phys. Soc. Japan* **58** 2515
[18] Tyablikov S V 1967 *Methods in the Quantum Theory of Magnetism* (New York: Plenum) sections 5, 35
Praveczki E 1963 *Phys. Lett.* **6** 147
Callen H B 1963 *Phys. Rev.* **130** 890